



# ICME Framework for Damage Assessment and Remaining Creep Life Prediction of In-Service Turbine Blades Manufactured with Ni-Based Superalloys

Chao Fu<sup>1</sup> · Yadong Chen<sup>1,2</sup> · Siliang He<sup>1</sup> · Stoichko Antonov<sup>1</sup> · Longfei Li<sup>1</sup> · Weiwei Zheng<sup>1</sup> · Qiang Feng<sup>1</sup>

Received: 8 August 2019 / Accepted: 22 October 2019 / Published online: 4 November 2019  
© The Minerals, Metals & Materials Society 2019

## Abstract

Accurate creep life prediction is necessary for the evaluation of the remaining creep lives of in-service turbine blades and for the design of new turbine blades in aircraft engines. In this study, an integrated computational material engineering methodology for predicting the remaining creep life of in-service turbine blades was developed by taking a microstructural criterion and creep strain criterion into consideration, and combining artificial neural networks with a modified  $\theta$  projection model to assess the service temperature, stress, degradation time, and existing creep strain. To explore the application of the method and verify its accuracy, the microstructural degradations at different locations of two directionally solidified superalloy DZ125 turbine blades, which were in-service for 300 h and 980 h in different engines, were characterized and quantified. Using these results, the remaining creep life of the microstructures at different locations of the blade was predicted. Finally, these creep life prediction results were experimentally verified using miniature creep test specimens. The development of this new method provides a reference for the design and service evaluation of turbine blades made of directional solidified and single-crystal Ni-based superalloys.

**Keywords** Turbine blades · Ni-based superalloy · ICME · Remaining creep life prediction · Miniature creep test

## Introduction

Turbine blades of aircraft engines, typically manufactured of Ni-based superalloys, are constantly exposed to high temperature and centrifugal loading during service, thereby activating creep deformation as the primary damage mode [1, 2]. In recent decades, there has been an increasing interest in accurate estimation of remaining creep life of turbine blades as a means of extending their service life, thus

reducing costs of manufacture and maintenance. Commonly, a critical creep strain, such as 1%, is set as an indicator or criterion for blade failure as part of the aeroengine's design specifications. Therefore, most of the existing creep life prediction models, including the  $\theta$  projection model and some TTP methods, are established based on the relationship among creep strain, creep temperature, stress, and time [3–6]. However, due to the sophisticated internal cooling passageway system and the blade's shape, the spatial distribution of the actual service temperature, stress and local creep strain for the turbine blades is very complex and difficult to determine [7, 8]. Additionally, the complex service history (non-isothermal and changing loads along the blade) also leads to complicated temporal distribution of the service conditions and level of microstructural degradation [9, 10]. Some researchers have pointed out that the worst (most demanding) condition lasts only 20% of the service total time; however, it results in substantial degradation of the turbine blades' mechanical properties [10]. Taking all of these factors into consideration, it becomes very challenging to

✉ Longfei Li  
lilf@skl.ustb.edu.cn

✉ Qiang Feng  
qfeng@skl.ustb.edu.cn

<sup>1</sup> Beijing Advanced Innovation Center for Materials Genome Engineering, State Key Laboratory for Advanced Metals and Materials, University of Science and Technology Beijing, Beijing 100083, China

<sup>2</sup> Department of General Technology, China North Vehicle Research Institute, Beijing 100072, China

determine the degree of degradation of the whole blade, and to accurately estimate or assess the remaining creep life of a turbine blade.

In general, attempting to determine the service conditions and the degradation distribution has become the most important step in different approaches for estimating the remaining creep life of turbine blades. For in-service turbine blades, even with complicated service history, the microstructural degradation is the most accessible information that can be captured directly by sectioning the blades during overhauls, and hence, assessing the degree of service degradation based on the microstructural evolution has become a popular method [11, 12]. Generally, creep degradation commonly consists of a decrease in the volume fraction and/or rafting of the  $\gamma'$  phase, decomposition of carbides and precipitation of TCP phases [13–17]. In addition, the formation of dislocation networks and the growth of stacking faults also significantly accelerate the creep cavity nucleation [18–20].

It should additionally be noted that a thin-wall effect should be taken into consideration as the cross-sectional area of a turbine blade's airfoil is significantly thinner than the standard bar specimens typically used to evaluate creep properties and estimate or assess the remaining creep life of turbine blades. The thin-wall effect is usually a consequence of the ratio of load-bearing area to thickness of the oxidation layer forming during creep. Since the oxide structure thickness is constant, reducing the sample thickness translates into a reduction in the load-bearing area, and although negligible for thicker cross sections, the oxide thickness becomes a substantial part of the load-bearing area for thin foils, effectively reducing creep performance [21–23].

Combining information on the macro- and microscale within an integrated computational materials engineering (ICME) approach may be an effective way to establish a reliable creep life prediction model for in-service turbine blades. In this study, a microstructure criterion for evaluating the service degradation degree of DZ125 turbine blades was determined. Based on this criterion and the work of our previous studies [24–27], a method for evaluating service degradation and predicting the remaining creep life of directionally solidified DZ125 turbine blades was developed. Finally, two DZ125 turbine blades after about 300 h and 980 h of service were characterized, and the remaining creep lives of these two blades were predicted and verified using the proposed method. It should be pointed out that the actual service state of turbine blades including creep, fatigue and interaction with environmental factors is always complex;

therefore, to simplify the analysis, only the creep degradation was considered in this study.

## Experimental

Two turbine blades were obtained from two different aircraft engines after 300 h and 980 h. During the service, the blades had been inspected at regular intervals (about every 300 h) and no rejuvenation treatment was implemented. The turbine blades were manufactured from a directionally solidified superalloy DZ125, which has been developed based on René DS 125 superalloy with a reduction in Ti and C and an increase in the Hf contents [28]. The chemical composition of DZ125 superalloy, which was measured by physicochemical phase analysis, is listed in Table 1. It should be noted that 1–3 turbine blades are generally removed and dissected to check the degradation degree during overhauls. Therefore, detailed characterization of the microstructural degradation is necessary and of benefit to the other blades in the turbine [29].

To evaluate the microstructural degradation of these two turbine blades, microstructural characterization was performed at six different locations. Meanwhile, miniature creep specimens were also sectioned from equivalent locations on the two blades and used to verify the remaining creep life predictions. The locations of all samples, including two on the pressure side and four on the suction side, are marked as 1 to 6 on the turbine blade shown in Fig. 1a. In addition, to obtain similar microstructures to the various locations of the blades and determine the microstructural criterion for assessing the degradation degree of DZ125 superalloy, various pre-treatment schemes, consisting of interrupted creep tests and aging, were conducted on standard heat-treated material.

Metallographic specimens (turbine blades and pre-treated specimens) were mechanically polished and then electrolytically etched using a 12% phosphate, 40% nitric acid and 48% sulfuric acid solution with a current of ~0.1 A for 3–5 s; this etching allows for the observation of  $\gamma'$  precipitates. The  $\gamma/\gamma'$  phase examination was performed using a ZEISS SUPRA 55 field-emission scanning electron microscope (FE-SEM). Using multiple images for statistical purposes, the quantitative analysis of the microstructural degradation included the characterization of  $\gamma'$  volume fraction ( $V_V$ ),  $\gamma'$  rafting degree ( $\Omega$ ) and thickness of the rafted  $\gamma'$  precipitates ( $D$ ). Details of the measurement methods for all these parameters

**Table 1** Measured chemical composition of the directional solidified DZ125 superalloy, wt%

Ni	Co	Cr	Al	Hf	Mo	Ta	W	Ti	C	B
Bal.	10.18	8.78	5.23	1.40	2.15	3.61	6.97	1.02	0.11	0.012

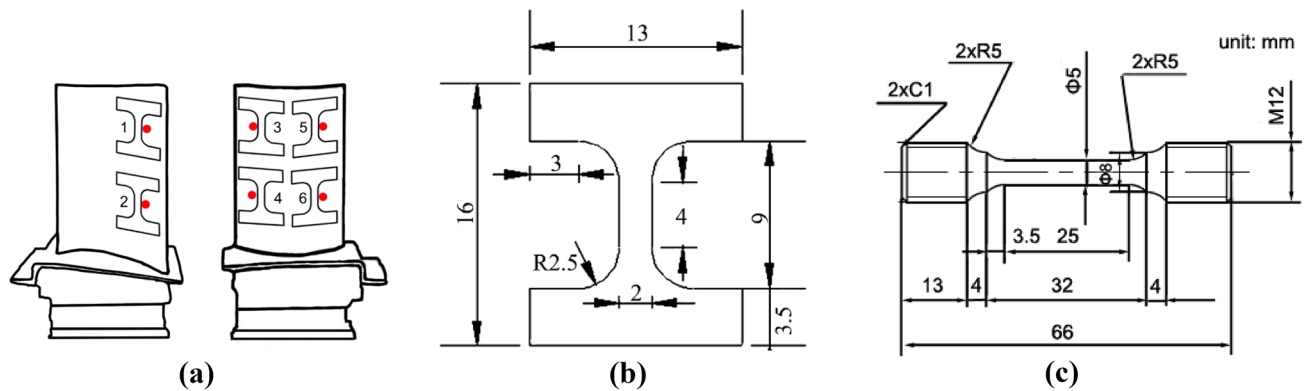


**Fig. 1** Experimental method for the analyses of turbine blades **a** illustration of the miniature creep sampling locations and the locations of a turbine blade for microstructural observation, **b** the sketch of the miniature creep test sample, **c** the sketch of the normal stress rupture test sample

can be found in our previous studies [24, 25]. These three parameters,  $V_f$ ,  $\Omega$  and  $D$ , were specifically chosen for this study as all three proved to be closely related to the  $T$ - $\sigma$  coupling simulation conditions and vary significantly for different conditions (substantial variation to measure changes) [24, 25]. All three descriptors are one dimension and can be easily obtained by simple stereological methods (easy to measure from the obtained images). Although different other microstructural features can also be considered (especially for different alloys/conditions), these three were deemed most appropriate with highest ease of measurement for the purposes of this study.

The sketch of the miniature creep specimen used to verify the results of the remaining creep life prediction is shown in Fig. 1b. The whole size of the miniature specimen was 16 mm  $\times$  13 mm with a gauge size 4 mm  $\times$  2 mm; the thickness of the specimen was dependent on the actual turbine blade thickness. These samples were specifically chosen from positions on the blade that are as flat as possible and away from ribs, thereby lessening the necessity for significant machining (<0.3 mm for the grips, and no machining for the gauge sections). Additional stress rupture tests of the DZ125 superalloy with different initial microstructures were performed at 980 °C/220 MPa on specimens with geometrical dimensions shown in Fig. 1c. The stress rupture and creep tests were compliant with the Chinese Standard GB/T 2039-2012, which is similar to the International Standard ISO 204: 2009.

## Results and Discussion

### Microstructural Degradation in Serviced Turbine Blades

The morphology of the  $\gamma'$  precipitates and  $\gamma$  matrix in the dendritic cores of the two turbine blades was examined by

FE-SEM to assess the degradation degree. Figure 2 shows the typical morphologies of the turbine blade that operated for 300 h at the different locations shown in Fig. 1a. In general, the morphology of the  $\gamma'$  precipitates at these six locations is close to cuboidal and very similar to the microstructure after the standard heat treatment (SHT) [24, 30]. Table 2 shows quantitatively characterized parameters ( $V_f$ ,  $\Omega$  and  $D$ ) for these locations. There are some differences among the examined locations, e.g., the  $V_f$  in location 1 (Fig. 2a1 and a2) is 58.9%, which is less than that in locations 2 to 6 (64.0–67.1%), and  $\Omega$  in location 1 is  $\sim$ 0.12, which is higher than those in locations 2 to 6 (0–0.08). The  $D$  values among the six locations are similar,  $\sim$ 420 nm. Hence, based on the morphology and microstructural parameters of the  $\gamma$  and  $\gamma'$  phases, the degradation at location 1 is more serious than in the other locations.

The typical  $\gamma/\gamma'$  morphology at the different locations (Fig. 1a) of the turbine blade that was in-service for 980 h is shown in Fig. 3. As expected, the microstructures show an obvious difference in morphology and size of the  $\gamma'$  precipitates, when comparing to corresponding locations of the 300-h blade. Additionally, the six examined locations in this turbine blade also show significant differences with each other. For instance, location 1 shows the most obvious  $\gamma'$  rafting and serious coarsening (Fig. 3a2), while the other locations show apparent coarsening, but no obvious rafting. The values of the quantitatively characterized parameters ( $V_f$ ,  $\Omega$  and  $D$ ) at the six locations of the 980-h blade are also listed in Table 2. The  $V_f$  values suggest that during service, there was a significant dissolution of  $\gamma'$  precipitates at locations 1 and 5, down to 43.7% and 51.8%, respectively, while the dissolution at the other locations was less significant and the  $V_f$  remained at a higher level (57.9–60.3%). Correspondingly, the  $\Omega$  at location 1 is 0.42, higher than at the other five locations. The  $D$  values at location 1, 5 and 6 are  $\sim$ 650 nm, while those at the other three locations

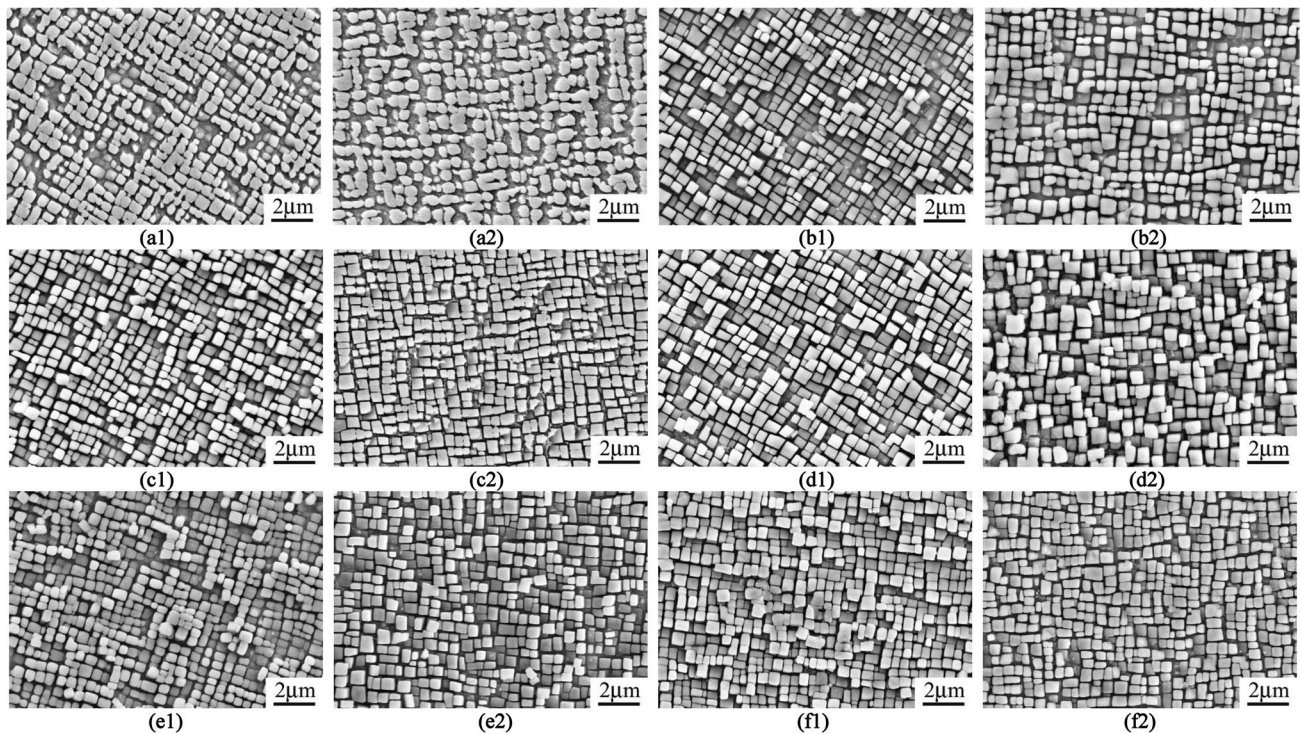


**Fig. 2** Typical  $\gamma/\gamma'$  morphologies in DZ125 turbine blade after service for 300 h **a** location 1, **b** location 2, **c** location 3, **d** location 4, **e** location 5, **f** location 6, (1) cross section, (2) longitudinal section

**Table 2** Microstructural parameters of two in-service DZ125 turbine blades

Locations	In-service for 300 h			In-service for 980 h		
	$V_f$ (%)	$\Omega$	$D$ (nm)	$V_f$ (%)	$\Omega$	$D$ (nm)
1	58.9	0.12	420	43.7	0.42	660
2	65.0	0.08	430	57.9	0.16	600
3	67.1	0.05	420	60.1	0.16	550
4	67.1	0	420	60.3	0.13	550
5	64.0	0	410	51.8	0.11	660
6	66.3	0	410	58.7	0.09	650

are ~ 550–600 nm. Based on these results, it can be concluded that location 1 shows the most significant degradation among the six examined locations, followed by location 5.

In brief, the degradation degree of the two turbine blades with different service history and service time was assessed based on the microstructural evolution of the  $\gamma/\gamma'$  microstructure. The results showed that the 300-h blade suffered light degradation in all the examined locations, while the 980-h blade showed more serious degradation at some locations. In the following sections, the degradation evaluation and the remaining creep life prediction of these two turbine blades are performed based on these microstructural characterization results.

### Microstructural Criteria for DZ125 Turbine Blades

As shown in our previous studies, quantitative characterization of the microstructure in-service turbine blades is a reliable method to evaluate their degradation degree [25]; however, it is not enough to further assess the temperature and stress during service. In industry, it is common practice to take a creep strain, such as 0.2% or 1%, as a simple indicator of the degradation level of the whole turbine blade. Nevertheless, it is very difficult to directly gauge the creep deformation of in-service turbine blades with sophisticated shape, especially for determining the local deformation. Therefore, finding a criterion based on the microstructure as the indicator for the degradation degree is a more direct



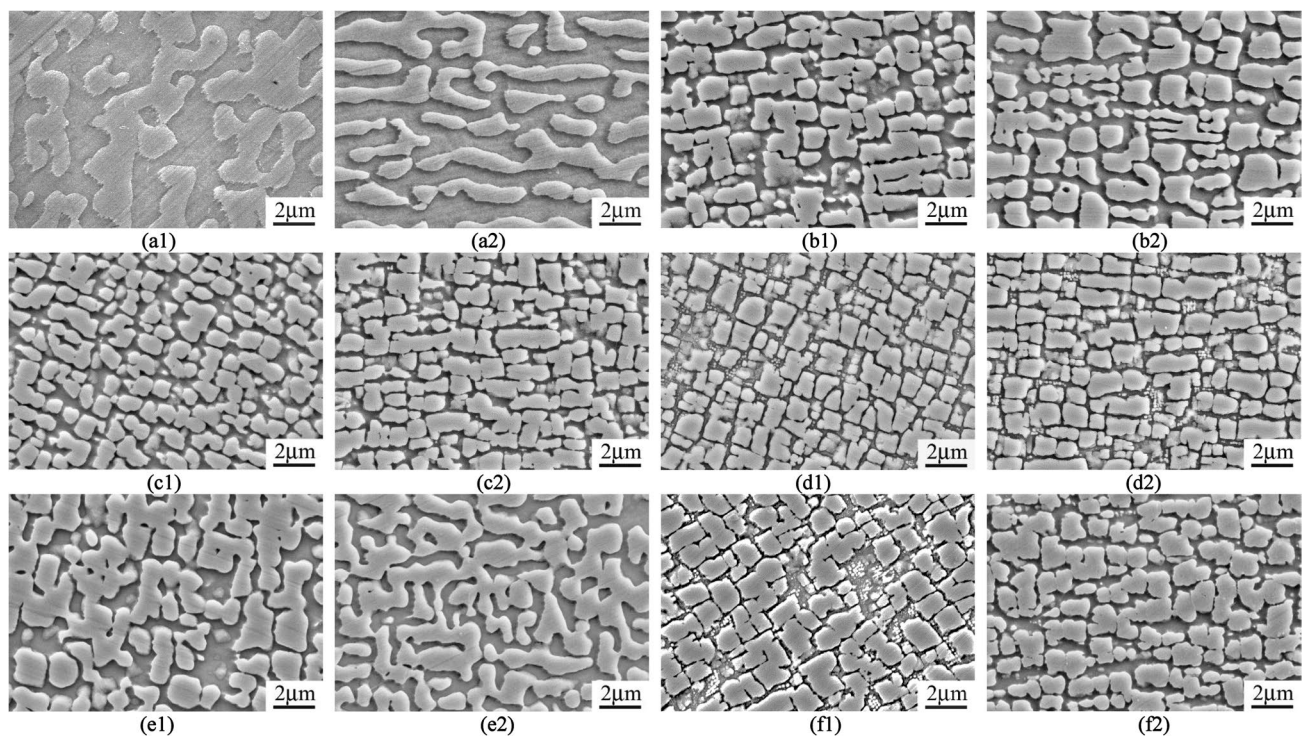


**Fig. 3** Typical  $\gamma/\gamma'$  morphologies in DZ125 turbine blade after service for 980 h **a** location 1, **b** location 2, **c** location 3, **d** location 4, **e** location 5, **f** location 6, (1) cross section, (2) longitudinal section

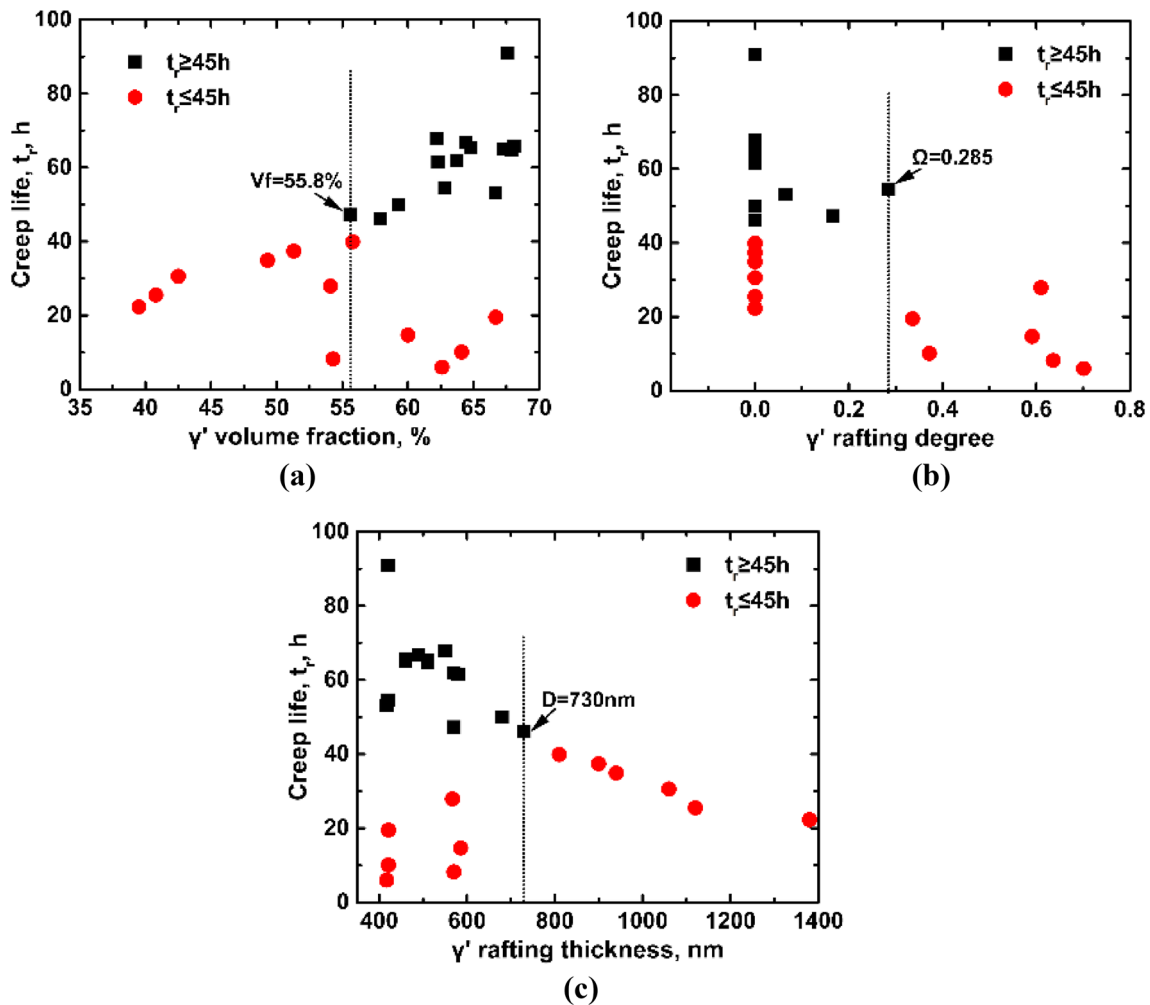
and powerful approach, as the microstructural parameters are easily quantifiable.

In this study, an effort was made to find a suitable microstructural criterion using the obtained turbine blades made of DZ125. According to the China Aeronautical Materials Handbook [28], the industrial requirement for the stress rupture property of DZ125 is that the creep rupture life should be above 32 h at 980 °C/235 MPa, or equivalently 45 h at 980 °C/220 MPa. As such, a database for pre-treatment conditions, initial microstructural parameters and the corresponding stress rupture life at 980 °C/220 MPa was built and is shown in Table 3. For a more intuitive interpretation, the results of Table 3 are plotted in Fig. 4. From these figures, it follows that for a creep rupture life higher than 45 h, the  $\gamma'$  volume fraction should be higher than 55.8%, and  $\gamma'$  thickness should be less than 730 nm with low rafting degree ( $\Omega \leq 0.285$ ). On the other hand, when these three microstructural parameters do not all meet the requirement above, the corresponding rupture life at 980 °C/220 MPa is almost always lower than 45 h, meaning that a blade with such a microstructure cannot continue service. Therefore, this microstructural criterion, obtained by analyzing the microstructures after creep simulations, can serve as a reference for evaluating the damage degree of in-service DZ125 turbine blades.

In “**Microstructural Degradation in Serviced Turbine Blades**” section, the microstructures of the two turbine blades in-service for 300 h and 980 h were characterized and the microstructural parameters were quantified. The 300-h blade meets the microstructural criterion, as the  $\gamma'$  rafting degree at the six investigated locations is lower than 0.285, while  $V_f$  is  $\geq 55.8\%$  and  $D$  is  $\leq 730$  nm (Table 2). Accordingly, the assessment results show that the degradation degree of the 300-h blade is relatively slight. However, the degradation at equivalent locations of the 980-h blade is more severe and complicated, as shown in Table 2. The microstructure in location 1 shows an obvious  $\gamma'$  rafting degree ( $\Omega = 0.42$ ), which is much higher than the criterion, 0.285. At the same time, the microstructure at location 5 shows slight  $\gamma'$  rafting ( $\Omega = 0.11$ ), but with a lower  $\gamma'$  volume fraction ( $V_f = 51.8\%$ ), again below the criterion. Therefore, among the examined 6 locations of the blade, the microstructures at location 1 and location 5 cannot satisfy the microstructural criterion and are unsuitable for further service; meanwhile, the microstructures at the other four locations meet the microstructural criterion and can continue service.

**Table 3** Pre-treatment, initial microstructural parameters and the corresponding stress rupture lives of the directional solidified DZ125 superalloy under 980 °C/220 MPa

Pre-treatment	$V_f$ (%) / $\Omega/D$ (nm)	$t_r$ (h)	Pre-treatment	$V_f$ (%) / $\Omega/D$ (nm)	$t_r$ (h)
SHT	67.6/0/420	90.9	1000 °C/84 MPa/100 h	62.8/0.542/420	54.6
900 °C/0 MPa/300 h	68.1/0/460	65.8 ± 8.8	1000 °C/84 MPa/300 h	60.0/0.591/586	14.7
900 °C/0 MPa/600 h	67.9/0/510	64.8 ± 3.2	1000 °C/110 MPa/100 h	62.6/0.701/417	6
900 °C/0 MPa/900 h	67.3/0/460	65.0 ± 2.3	1050 °C/0 MPa/100 h	62.3/0/580	61.6
900 °C/294 MPa/100 h	66.7/0.336/421	19.5	1050 °C/0 MPa/300 h	55.8/0/810	39.9 ± 3.8
900 °C/350 MPa/25 h	66.7/0.065/417	53.1	1050 °C/0 MPa/600 h	51.3/0/900	37.4 ± 8.4
950 °C/0 MPa/300 h	64.4/0/490	66.8 ± 9.3	1050 °C/0 MPa/900 h	49.3/0/940	34.9 ± 3.3
950 °C/0 MPa/600 h	64.8/0/510	65.4 ± 4.4	1050 °C/18 MPa/100 h	55.6/0.166/570	47.3
950 °C/0 MPa/900 h	63.7/0/570	61.9 ± 6.3	1050 °C/53 MPa/100 h	54.1/0.610/567	27.9
950 °C/162 MPa/100 h	64.1/0.372/421	10.1	1050 °C/120 MPa/100 h	54.3/0.636/570	8.2
1000 °C/0 MPa/300 h	62.2/0/550	67.9 ± 13.2	1100 °C/0 MPa/300 h	42.5/0/1060	30.6 ± 0.1
1000 °C/0 MPa/600 h	59.3/0/680	49.9 ± 0.6	1100 °C/0 MPa/600 h	40.8/0/1120	25.5 ± 2.9
1000 °C/0 MPa/900 h	57.9/0/730	46.1 ± 6.0	1100 °C/0 MPa/900 h	39.5/0/1380	22.3 ± 3.4

**Fig. 4** Relationship of stress rupture lives of DZ125 superalloy with different microstructure parameters a  $\gamma'$  volume fraction versus creep life, b  $\gamma'$  rafting degree vs creep life, c  $\gamma'$  rafting thickness versus creep life

## Procedures for Remaining Creep Life Prediction

In this study, a new approach for predicting the remaining creep lives of in-service turbine blades is developed on the basis of microstructural parameters required for a minimum creep life and taking into consideration the microstructural evolution and creep strain. The specific steps for determining the remaining creep life of a turbine blade are summarized in Fig. 5. In general, the approach entails four steps:

- (i) Microstructural observation and quantitative characterization

The microstructures at different locations of a turbine blade after service should be analyzed. For the DZ125 turbine blades in this study, the  $\gamma/\gamma'$  structure in the cross and longitudinal sections was observed as outlined above, and subsequently, the specific microstructural parameters ( $V_{\gamma'}$ ,  $\Omega$  and  $D$  in this case) were quantified.

- (ii) Service condition assessment

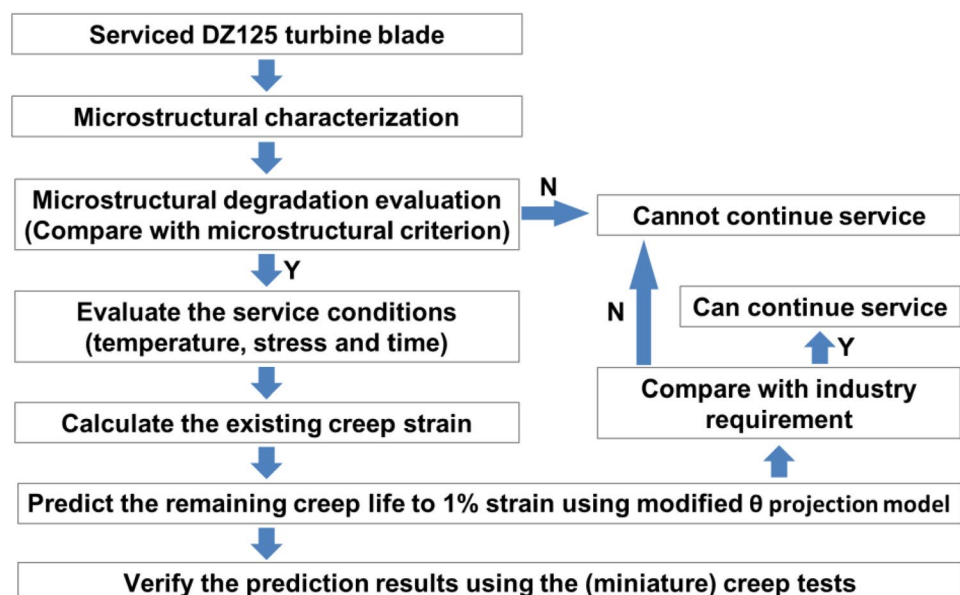
The service condition distribution, including temperature, stress and degradation time, in different locations of the turbine blade can be assessed based on the microstructural parameters using a back-propagation artificial neural network (BPANN) model, which was established in another study [31]. To establish this BPANN model, 138 sets of experimental data were used, 97 of which, i.e., 70% of all data, were used as the training data, 17 sets were used as validation data, and the remaining 24 sets were used as the testing data. As for the hyperparameters of the artificial neural network, including the number of hidden layers of the model and the number of

neurons, they are mainly comparing different models and setups. As there are different types of machine learning models, which may be suitable to resolve the complex relationships between microscopic organization and macroscopic parameters, we compared the predicted accuracy of different models, including BPANN (ANN), random forest, support vector machine and gradient boosting, and the detailed results are also shown in Ref. [31]. We found that the highest precision (in terms of lowest prediction error) is obtained when using the BPANN model.

It is noteworthy that in contrast to the standard creep test samples, turbine blades suffer more complicated loading conditions during service at the temporal and spatial levels, due to the complex service history of aeroengines and the intricate shape of the turbine blades [7]. Therefore, this study proposes the equivalent worst service condition, where the service temperature, stress and time evaluated for a given microstructure represent the worst service situation that causes the major degradation to achieve this microstructure.

In order to obtain the service temperature, stress and time evaluation results for each microstructural parameter, two ANN models for simultaneously evaluating the temperature and stress with different input parameters are proposed, as shown in Fig. 6. The structure and the hyperparameters of the models were determined by a trial and error method. Figure 6a assesses the temperature and stress based on the creep time ( $t$ ),  $\gamma'$  volume fraction ( $V_{\gamma'}$ ) and  $\gamma'$  rafting degree ( $\Omega$ ), while Fig. 6b uses the creep time ( $t$ ),  $\gamma'$  rafting thickness ( $D$ ) and  $\gamma'$  rafting degree ( $\Omega$ ). By

**Fig. 5** Procedures for the remaining creep life prediction of in-service turbine blades



varying the degradation time ( $t$  in Fig. 6) input, the evaluated temperature and stress will change even for the same microstructural parameters. Once the correct degradation time is selected, the evaluated creep temperature and stress for the two ANN models will be equal, and the corresponding results are deemed as the equivalent worst service condition (including temperature, stress and time). For example, Fig. 7 shows the evaluated temperature and stress at different degradation time (keeping the microstructural parameters constant). The temperature and stress obtained from the two models are both equal to 1000 °C and 70 MPa, respectively, when the degradation time is about 120 h, and this is deemed as the equivalent worst service condition for a microstructure described by these particular parameters.

(iii) Degradation evaluation

The degradation at the micro- and macroscales can be evaluated based on the above results. Specifically, the microstructural parameter obtained in step (ii) is first compared with the microstructural criterion to gauge the relative microscale degradation. In this way, the microstructures can be subdivided into two parts: one that meets the criterion and one that does not. In addition, once the service temperature, stress and degradation time are obtained in step (ii), the creep strain of the particular location can be evaluated by the modified  $\theta$  projection model [26, 27] using Eqs. (1) and (2).

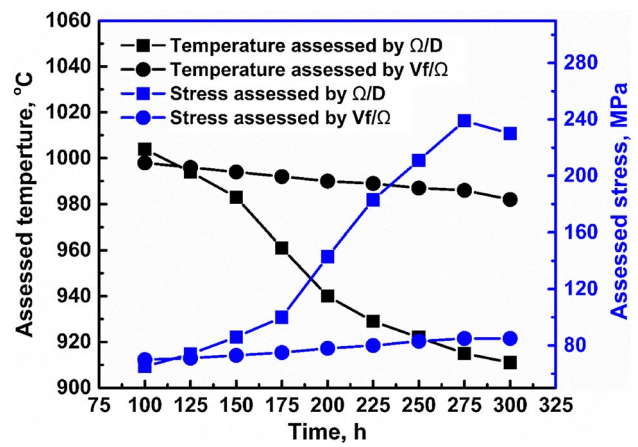


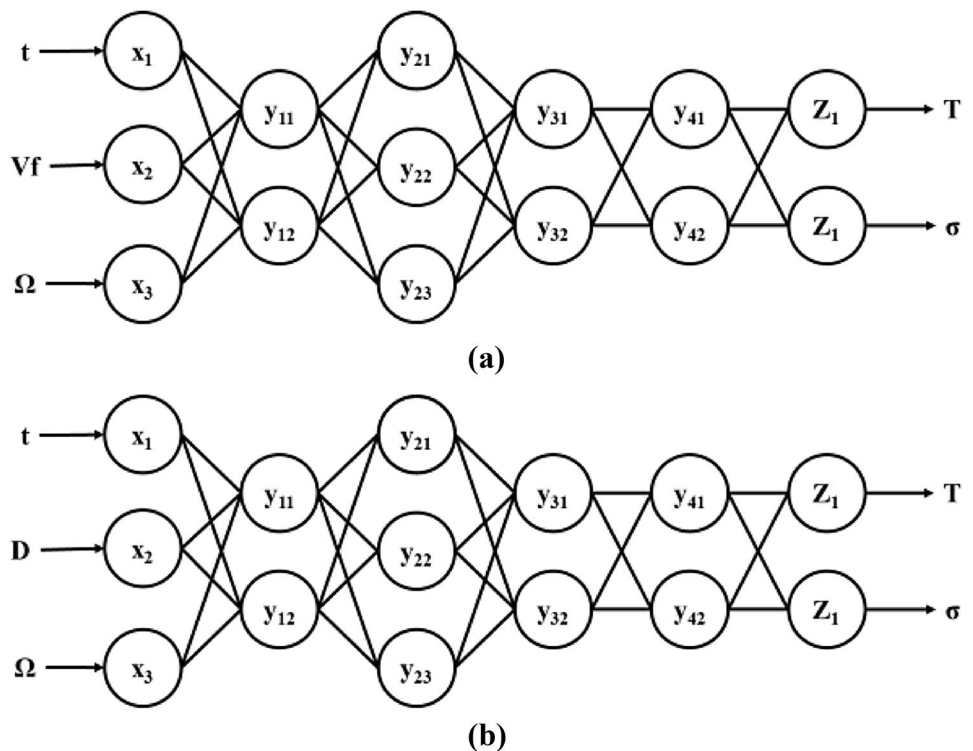
Fig. 7 Evaluation results of temperature and stress in different degradation time assessed by  $\gamma'$  volume fraction ( $V_f$ )/ $\gamma'$  rafting degree ( $\Omega$ ) and  $\gamma'$  rafting thickness ( $D$ )/ $\gamma'$  rafting degree ( $\Omega$ ), respectively

$$\varepsilon = \theta_1 (1 - e^{-\theta_2 t}) + \theta_3 (e^{\theta_4 e^{\theta_5 t}} - 1) \tag{1}$$

$$\log \theta_i = a_i + b_i \sigma_0 + c_i T + d_i \sigma_0 T \quad (i = 1, 2, 3, 4, 5) \tag{2}$$

where  $\varepsilon$  is the creep strain and  $t$ ,  $\sigma_0$  and  $T$  are, respectively, the creep time, initially applied creep stress and creep temperature (obtained from step (ii)); the parameters  $\theta_i$ , for  $i = 1, 2, 3, 4$  and  $5$ , are determined by the regression of the creep curves; and  $a_i$ ,  $b_i$ ,  $c_i$

Fig. 6 ANN models for service conditions based on different input parameters **a** input parameters: creep time ( $t$ ),  $\gamma'$  volume fraction ( $V_f$ ),  $\gamma'$  rafting degree ( $\Omega$ ), **b** input parameters: creep time ( $t$ ),  $\gamma'$  rafting thickness ( $D$ ),  $\gamma'$  rafting degree ( $\Omega$ )





and  $d_i$  for  $i = 1, 2, 3, 4$  and  $5$  are material constants. By comparing the calculated creep strain ( $\epsilon$ ) with the creep strain criterion, such as 1%, the degradation at the macroscale can also be assessed. It should be pointed out the  $\theta$  projection model for DZ125 has been already established using 6 creep curves, obtained by standard specimens, under different conditions within 0–10% creep strain in our previous study [26, 27].

(iv) Remaining creep life prediction and verification

The remaining creep life of turbine blades that meet both the microstructural and macrocriterion would be predicted. In this study, the remaining creep lives are predicted using the modified  $\theta$  projection model a creep strain criterion of 1% strain. In addition, to obtain an accurate prediction result, the thin-wall effect is taken into account. That is, the remaining life to 1% creep strain ( $t_e$ ) equals to the product of the modified  $\theta$  projection model prediction and a scaling factor for the thin-wall effect. More details on thin-wall scaling factor used in this study are provided in “Application of the Remaining Creep Life Prediction Method” section. Finally, comparing the obtained result with the industrial requirement from the handbooks, it can be determined whether the other turbine blade in the engine can continue servicing.

To provide a case study, the predicted creep lives of the two turbine blades were verified at the corresponding creep conditions using miniature creep specimens sectioned from the turbine blades.

### Application of the Remaining Creep Life Prediction Method

The remaining creep lives of the two investigated turbine blades could be predicted based on the procedure proposed

in “Procedures for Remaining Creep Life Prediction” section, and using the quantitatively characterized microstructural parameters in “Microstructural Degradation in Serviced Turbine Blades” section and microstructural criterion established in “Microstructural Criteria for DZ125 Turbine Blades” section. The evaluated equivalent worst service temperature and stress, as well as the corresponding degradation time, for the different locations of the 300-h and 980-h turbine blades are shown in Table 4. For the 300-h turbine blade, the service temperatures were roughly in the range of 910–1020 °C, with equivalent stresses of 60 to 185 MPa and equivalent degradation times of ~25 to 50 h. For the different locations of the 980-h turbine blade, the service temperatures were roughly in the 1010–1090 °C range, with equivalent stresses of 10 to 20 MPa and equivalent degradation times of ~100 to 530 h. Based on the evaluation results of the service condition (including temperature, stress and degradation time), it can be deduced that the lower  $V_f$  in location 1 and location 5 of the 980-h turbine blade was caused by a high service temperature (1080–1090 °C), while a lower service temperature led to just a slight degradation at the other four locations.

From the evaluation results of the service conditions, the existing creep strains ( $\epsilon_e$ ) at different locations were also calculated using Eqs. (1) and (2) and are listed in Table 4. The results show that the creep strains at the different locations of the two investigated turbine blades were very small due to the low service temperature (for the 300-h blade), stress (for the 980-h blade) and degradation time. Although the estimated creep strains at the different locations of the 980-h blade were much smaller than 1%—meeting the macrocriterion, the microstructural evaluation results shown in Table 2 indicate that the 980-h blade could not meet the microcriterion due to severe microstructural degradations at locations 1 and 5 (Fig. 3a and e). Therefore, this blade cannot continue service, and the remaining creep life prediction and verification were only conducted for the 300-h blade.

**Table 4** The prediction results of the service conditions for the two in-service DZ125 turbine blades and the remaining creep life to 1% creep strain ( $t_e$ ) under 980 °C/220 MPa for the 300-h serviced turbine blade

Blades (h)	Locations	$T$ (°C)	$\sigma$ (MPa)	$t$ (h)	$\epsilon_e$ (%)	$t_e$ (h)	$t_{\text{test}}$ (h)
300	1	~1020	~61	25–50	~0.10	~14	10.2
	2	~980	~91	25–50	~0	~15	13.3
	3	~910	<185	<25	~0	~15	
	4	~910	<125	<25	~0	~15	
	5	~980	~63	25–50	~0.06	~14	
	6	~940	~105	25–50	~0	~15	
980	1	~1090	~20	100–125	0.13	–	
	2	~1045	~11	150–175	0.05	–	
	3	~1015	~7	200–225	~0	–	
	4	~1015	~7	200–225	~0	–	
	5	~1080	~8	150–175	0.06	–	
	6	~1010	~20	480–530	~0	–	

As mentioned previously, before predicting the remaining creep life, a scaling factor to account for the thin-wall effect for the specific alloy/airfoil needs to be determined first. Figure 8 shows the creep strain–time curves of specimens with different cross-sectional areas. The results show that the rupture life for a 1 mm\*2 mm cross-sectional area sample is about 55 h, which is ~60% that of the standard specimen ( $\Phi$  5 mm), consistent with a previous report [22]. Additionally, the time to 1% strain of the miniature specimen is about 14–15 h vs. 26 h of the standard one. Thus, predicting the remaining life should take this thin-wall effect into account; otherwise, using the creep strain as the criterion may result in an overestimation. It should be noted that little to no machining was needed to completely flatten the miniature samples, depending on their location on the blade. This effectively will slightly reduce the thickness ( $<0.05$  mm), as compared to that of the original blade, and therefore increase the scaling factor by a small amount. This increase can be taken as a safety margin as it will result in underestimation of the predicted life. With this in mind, the influence factor for the thin-walled effect for predicting the remaining life to 1% strain under 980 °C/220 MPa using modified  $\theta$  projection model was set as 0.6, which was deemed appropriate based on the comparison of miniature and standard creep specimens. Using this scaling factor, the remaining creep life to 1% creep strain ( $t_e$ ) under 980 °C/220 MPa of the 300-h blade were predicted, and the prediction results are also listed in Table 4. The remaining creep lives at the six locations are very close to each other, ~14–15 h, due to the slight degradation at each location of this blade as well as the low service temperature and stress.

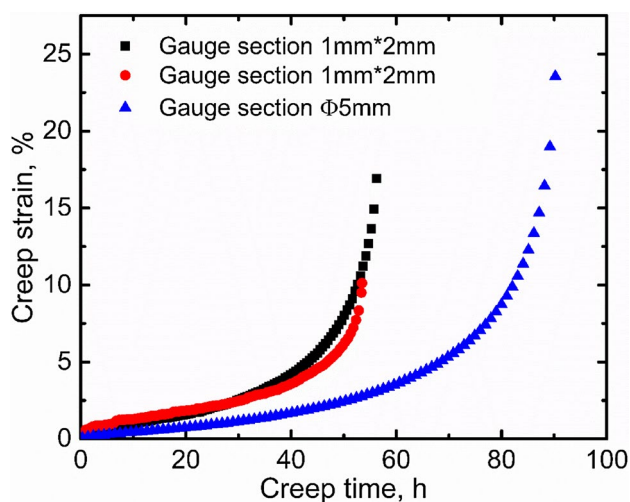


**Fig. 8** Creep strain–time curves of the specimens sectioning from un-serviced DZ125 turbine blade (section area 1 mm\*2 mm) and the standard specimen (section area  $\Phi$  5 mm) under 980 °C/220 MPa

To verify these creep life predictions, creep tests of the miniature specimen from the different locations of the 300-h serviced turbine blade were conducted under 980 °C/220 MPa. Figure 9 shows the creep curves of the samples from location 1 and location 2, where the microstructures experienced the worst degradation. First, the rupture lives of these two locations are 30 h and 46 h, respectively, both longer than the product of industrial criterion for the standard specimen and the impact factor of thin-wall effect, i.e.,  $45 \text{ h} \times 0.6 = 27 \text{ h}$ , suggesting that the 300-h turbine blades still meet the industrial requirements for the stress rupture property of DZ125 superalloy. Second, the remaining creep life to 1% strain at these two locations, as obtained from the curves, is 10.2 h for location 1 and 13.3 h for location 2 (Table 4), portraying that the prediction results are accurate enough. Finally, based on the creep test results of the worst degraded locations, the other 300-h turbine blades in the engine are considered to be able to continue service.

## Applicability and Limitations

In industrial applications, the overall deformation of the blade and the amount of local deformation are generally used as indicators for judging whether the blade can continue service. In this study, we took the local microstructure and the local creep strains, which are more difficult to measure, but more accurate, as the life prediction criterion. During typical engine overhaul, one to three turbine blades are pulled out of the engine and dissected and analyzed. The

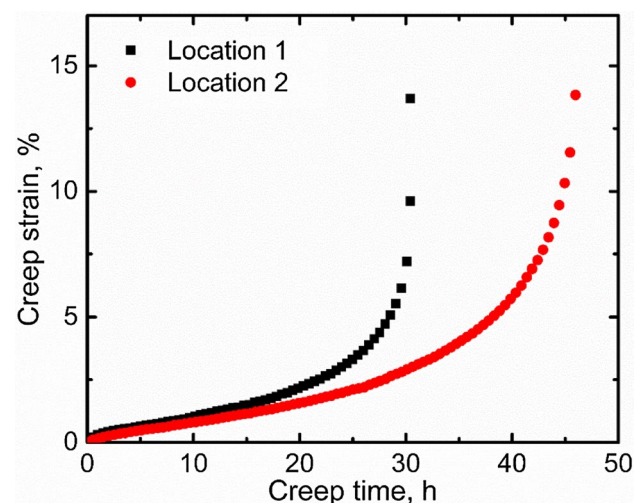


**Fig. 9** Creep strain–time curves of the specimens sectioning from locations 1 and 2 in the 300-h serviced turbine blade under 980 °C/220 MPa

method established in this paper is based on this practice, where the obtained turbine blades are extensively analyzed in aim to guide the subsequent service assessment of other turbine blades.

This study took into consideration the drawbacks of the existing models for both service evaluation and creep life prediction of turbine blades and proposes an optimized methodology within an ICME framework. First, the developed approach is aimed at predicting the remaining creep life not only of SHTed specimens, but also for samples with degraded microstructures, which extends its capability to actual in-service turbine blades. Second, it is always challenging to gauge the degree of degradation of in-service turbine blades; hence, the proposed approach introduces microstructural parameters that can be directly evaluated by sectioning a blade during overhaul and that correlate to a degradation degree. Finally, this method considers micro-scale as well as the macroscale features that lead to reduction in the creep properties. As creep damage accumulates, both microstructural degradation and creep strain accumulation to a certain degree are unavoidable. For instance, heavy degradation of the microstructure accompanied by small creep strain typically occurs at high temperature and low stress conditions, and vice versa. Therefore, it is necessary to take both the microstructure and the accumulated creep strain into consideration when predicting the remaining life. The proposed new method in this study provides the possibility to accurately gauge the level degradation of in-service turbine blades regardless of the service history and to use that information to predict the remaining creep life. This will also benefit the engine overhaul timing and lifetime extension of turbine blades in the aviation industry.

Nevertheless, there are still some limitations or drawbacks of the proposed method that should be pointed out. First, all of the assessment and predictions are established based on the microstructural evolution, as quantified by three parameters. However, in order to more accurately represent the microstructural evolution, it is necessary to develop a more efficient method for microstructural description. Second, the database for the machine learning models in this study was established using experimental data; however, conventional creep tests are not easy to conduct due to complex testing procedures and high associated costs. Moreover, such data are alloy specific and cannot be used for say a newer generation alloy. Therefore, it is also necessary to find novel ways to populate databases, such as high-throughput creep testing and new machine learning models. Finally, as mentioned above, more complex service conditions, such as creep–fatigue coupling and environmental factors, still need to be investigated systematically and incorporated into the method in the future for more reliable assessment results of in-service turbine blades.

## Conclusion

Microstructural degradation evaluation and remaining creep life prediction were conducted on turbine blades taken from different engines during overhaul, and an ICME method is proposed in this study. The main conclusions can be summarized as following:

1. According to the industrial standard, stress rupture tests were conducted on pre-treated specimen with different initial microstructures at 980 °C/220 MPa. A database of the results was built and, based on this a microstructural criterion of  $V_f \geq 55.8\%$ ,  $D \leq 730$  nm and  $\Omega \leq 0.285$ , was established to judge whether the turbine blades in the engine can continue service.
2. An ICME method for predicting the remaining creep life of in-service turbine blades was developed by taking the microstructural evolution and creep strain into consideration. This method consists of four steps: (1) microstructural observation and quantitative characterization; (2) service condition assessment; (3) degradation evaluation; and (4) remaining creep life prediction and verification. The remaining creep life of the turbine blades can be accurately predicted when the microstructural parameters are accurately quantified and a proper scaling factor for thin-walled effect is chosen.
3. The service degradation evaluation and remaining creep life prediction of two turbine blades were conducted within the methods framework, and the results were compared to experimental results, obtained by miniature creep specimens excised from the blades. The comparison shows that the creep life prediction methodology proposed in this study is reliable in accurately predicting the remaining creep life.

**Acknowledgements** The support provided by the National Key Research and Development Program of China (Grant No. 2016YFB0701403), the National Natural Science Foundation of China (Grant No. 51771019 and 51631008) and the 111 Project (No. B170003) is gratefully acknowledged.

## References

1. Antony KC, Goward GW (1988) Aircraft gas turbine blade and vane repair. In: Superalloys 1988, pp 745–754
2. AkeKarlsson S, Persson C, Persson PO (1995) Metallographic approach to turbine blade life time prediction. *Adv Manuf Process* 10(5):939–953
3. Larson FR (1952) A time temperature relationship for rupture and creep stress. *Trans ASME* 74:765–775
4. Manson SS, Haferd AM (1953) A linear time-temperature relation for extrapolation of creep and stress-rupture data. Technical Note 2890, NACA

5. Orr RL, Sherby OD, Dorn JE (1953) Correlations of rupture data for metals at elevated temperatures. Institute of Engineering Research, University of California, Berkeley
6. Manson S, Succop G (1956) Stress-rupture properties of Inconel 700 and correlation on the basis of several time-temperature parameters. In: Symposium on metallic materials for service at temperatures above 1600 F, ASTM International
7. Wen Z, Hou N, Wang B, Yue Z (2010) Crystallographic life model for single crystal turbine blade and validation by the miniature specimens cut from the turbine blades. *Multidiscip Model Mater Struct* 6(4):508–529
8. Dye D, Ma A, Reed RC (2008) Numerical modelling of creep deformation in a CMSX-4 single crystal superalloy turbine blade. In: *Superalloys 2008*. John Wiley & Sons, Inc., Champion, PA, pp 911–919
9. Pollock TM, Tin S (2006) Nickel-based superalloys for advanced turbine engines: chemistry, microstructure and properties. *J Propul Power* 22(2):361–374
10. Reed RC (2008) *The superalloys: fundamentals and applications*. Cambridge University Press, Cambridge
11. Miura N, Kondo Y (2011) Morphology of  $\gamma'$  precipitates in a first stage low pressure turbine blade of a Ni-based superalloy after service and after following aging. *J ASTM Int* 9(2):1–9
12. Miura N, Nakata K, Miyazaki M, Hayashi Y, Kondo Y (2010) Morphology of  $\gamma'$  precipitates in second stage high pressure turbine blade of single crystal nickel-based superalloy after serviced. *Mater Sci Forum* 638:2291–2296
13. Lvov G, Levit V, Kaufman M (2004) Mechanism of primary MC carbide decomposition in Ni-base superalloys. *Metall Mater Trans A* 35(6):1669–1679
14. Nathal M, MacKay R (1987) The stability of lamellar  $\gamma$ - $\gamma'$  structures. *Mater Sci Eng* 85:127–138
15. Qin X, Guo J, Yuan C, Chen C, Hou J, Ye H (2008) Decomposition of primary MC carbide and its effects on the fracture behaviors of a cast Ni-base superalloy. *Mater Sci Eng A* 485(1–2):74–79
16. Yuan X, Song J, Zheng Y, Huang Q, Yagi K, Xiao C, Feng Q (2016) Abnormal stress rupture property in K465 superalloy caused by microstructural degradation at 975 °C/225 MPa. *J Alloy Compd* 662:583–592
17. Cheng K, Jo C, Jin T, Hu Z (2011) Precipitation behavior of  $\mu$  phase and creep rupture in single crystal superalloy CMSX-4. *J Alloy Compd* 509(25):7078–7086
18. Carter TJ (2005) Common failures in gas turbine blades. *Eng Fail Anal* 12(2):237–247
19. Dubiel B, Czyska-Filemonowicz A (2012) TEM analyses of microstructure evolution in Ex-service single crystal CMSX-4 gas turbine blade. *Solid State Phenom* 186:139–142
20. Carroll L, Feng Q, Pollock T (2008) Interfacial dislocation networks and creep in directional coarsened Ru-containing nickel-base single-crystal superalloys. *Metall Mater Trans A* 39(6):1290–1307
21. Cassenti B, Staroselsky A (2009) The effect of thickness on the creep response of thin-wall single crystal components. *Mater Sci Eng A* 508(1–2):183–189
22. Doner M, Heckler JJS (1988) Identification of mechanisms responsible for degradation in thin-wall stress-rupture properties. In: *Superalloys 1988*, pp 653–662
23. Hüttner R, Gabel J, Glatzel U et al (2009) First creep results on thin-walled single-crystal superalloys. *Mater Sci Eng A* 510:307–311
24. Chen Y, Zheng Y, Xiao C, Feng Q (2016) Evaluation of temperature and stress in first stage high pressure turbine blades of a directionally-solidified superalloy DZ125 after service in aeroengines. In: *Superalloys 2016*. John Wiley & Sons, Inc., Hoboken, NJ, pp 701–710
25. Chen Y, Zheng Y, Feng Q (2016) Evaluating service temperature field of high pressure turbine blades made of directionally solidified DZ125 superalloy based on micro-structural evolution. *Acta Metall Sin* 52(12):1545–1556
26. Fu C, Chen Y, Yuan X, Tin S, Antonov S, Yagi K, Feng Q (2019) A modified  $\theta$  projection model for constant load creep curves-I. Introduction of the model. *J Mater Sci Technol* 35(1):223–230
27. Fu C, Chen Y, Yuan X, Tin S, Antonov S, Yagi K, Feng Q (2019) A modified  $\theta$  projection model for constant load creep curves-II. Application of creep life prediction. *J Mater Sci Technol* 35(4):687–694
28. Editorial Board of China Aeronautical Materials Handbook (2005) *China aeronautical materials handbook*. Standards Press of China, Beijing
29. Chunhu T (2008) *Failure analysis and prevention for rotor in aero-engine*. National Defense Industry Press, Beijing
30. Zhang J, Zheng YR, Feng Q (2016) Study on rejuvenation heat treatment of a directionally-solidified superalloy DZ125 damaged by creep. *Acta Metall Sin* 52(6):717–726
31. Chao F, Chen Y, Li L, Antonov S, Feng Q Exploration of quantitative correlation between microstructures and creep property of a directionally-solidified superalloy using ICME method. *J Alloys Compd* (under revision)